ELSEVIER

Biophysical Chemistry 128 (2007) 1 – 12

Biophysical Chemistry

http://www.elsevier.com/locate/biophyschem

Review

Structural insights of HutP-mediated regulation of transcription of the *hut* operon in *Bacillus subtilis*

Thirumananseri Kumarevel *

Biometals Laboratory and Advanced Protein Crystallography Research Group, RIKEN Harima Institute at SPring-8, 1-1-1 Kouto, Sayo-cho, Sayo-gun, Hyogo 679-5148, Japan

Received 12 January 2007; received in revised form 1 March 2007; accepted 1 March 2007
Available online 13 March 2007

Abstract

Regulating gene expression directly at the mRNA level represents a novel approach to control cellular processes in all organisms. In this respect, an RNA-binding protein plays a key role by targeting the mRNA to regulate the expression by attenuation or an anti-termination mechanism only in the presence of their cognate ligands. Although many proteins are known to use these mechanisms to regulate the gene expression, no structural insights have been revealed to date to explain how these proteins trigger the conformation for the recognition of RNA. This review describes the activated conformation of HutP, brought by the coordination of L-histidine and Mg^{2+} ions, based on our recently solved crystal structures [uncomplexed HutP, HutP–Mg^{2+}, HutP–L-histidine, HutP–Mg^{2+}–L-histidine, HutP–Mg^{2+}–L-histidine-RNA]. Once the HutP is activated, the protein binds specifically to bases within the terminator region, without undergoing further structural rearrangement. Also, a high resolution (1.48 Å) crystal structure of the quaternary complex containing the three GAG motifs is presented. This analysis clearly demonstrates that the first base in the UAG motifs is not important for the function and is consistent with our previous observations.

Keywords: HutP; Transcription regulation; Single strand RNA binding proteins; Attenuation; Anti-termination; Metal ions; Allosteric activation

Contents

1. Introduction

Bacteria exploit a variety of mechanisms to regulate transcription elongation, in order to control gene expression in response to changes in their environment. A frequently-used pathway involves the formation of a potential terminator

* Tel.: +81 791 58 2838; fax: +81 791 58 2835.
E-mail address: tskvel@spring8.or.jp.

0301-4622/$ - see front matter © 2007 Published by Elsevier B.V.
doi:10.1016/j.bpc.2007.03.003

structure upstream of the coding region, which functions in concert with activated cellular factors to terminate at that site or to allow transcription to proceed through it. In one case, the quiescent state allows transcription, and the binding of an activated factor activates the termination complex, causing transcription to abort. In the other, the ground state of the mRNA possesses a specific secondary structure capable of triggering the RNA polymerase to pause, prompting the release of both the polymerase and RNA transcript from the DNA template [1]. In this case, the binding of a *trans*-acting factor alleviates this block, allowing transcriptional read-through. This second process is generally referred to as an attenuation or an anti-termination mechanism of regulation. The distinction between these two pathways is the end-result of interactions between the terminator and the activated protein: is transcription terminated or allowed to continue? In the attenuation process, the regulatory protein, activated by the regulatory molecule, pauses the transcription at the terminator structure, which otherwise permits the read-through of the transcription apparatus. The best example for this kind of regulation is the tryptophan biosynthetic operon [2,3]. In contrast to this mechanism, the anti-termination process requires the activated protein to bind to the pre-existing terminator structure, to allow the RNA polymerase to transcribe the downstream genes. An example of this is the BglG/SacY family of anti-termination proteins [4,5] (Fig. 1). The target sequences for these anti-terminator proteins comprise either single- or double-stranded regions of their respective mRNAs.

In order to understand these mechanisms of attenuation and anti-termination in bacteria, so far we have only two protein–RNA complexes available. These are the TRAP attenuation protein and the LicT anti-termination protein. Surprisingly, both are from *Bacillus subtilis*. The TRAP protein regulates transcription of the *B. subtilis* tryptophan biosynthetic (*trp*) operon. TRAP is composed of 11 identical subunits arranged in a ring- shaped molecule. Upon activation by binding up to 11 L-tryptophan molecules, TRAP binds to an RNA target consisting of 11 GAG and UAG repeats in the 5′ leader region of the mRNA [6,7]. This binding inhibits formation of an anti-terminator structure, hence promoting formation of a terminator hairpin, which halts transcription in the trp leader region, upstream of the structural genes. Although the binary (Fig. 2a) and ternary complexes (Fig. 2b) of TRAP revealed the important interactions with the L-tryptophan and RNA, respectively, the structure in the absence of ligand (apo-TRAP) is not available to reveal insights into any structural rearrangements that might occur on binding to their respective ligands.

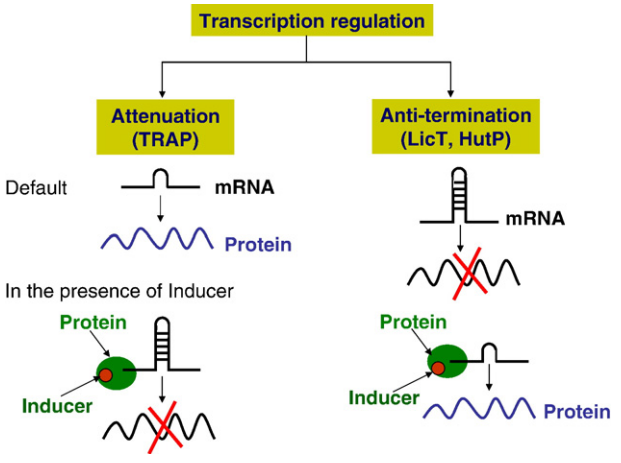

Fig. 1. Schematic representation of the transcription regulation by an anti-termination or attenuation mechanism. The difference between the attenuation and anti-termination has been delineated. In the absence of ligand binding (non-activation), transcription proceeds in the case of attenuation mechanism, and in contrast to this, anti-termination requires the activated protein.

LicT is a member of the BglG-SacY family of anti-termination proteins, which regulate transcription of genes involved in carbohydrate metabolism. These proteins bind to RNA targets known as RATs that consist of stem–loop structures, which overlap adjacent transcription terminators. Protein binding stabilizes the RAT structure, thereby inhibiting formation of the terminator. Apart from the N-terminal RNA binding domain (CAT), these proteins have two regulatory domains (PRD1 and PRD2), which contain sites for phosphorylation in response to carbohydrate availability. Recently, by comparing the native (inactive) and mutant (active) analyses of the LicT crystal structures showed massive tertiary and quaternary rearrangements of the entire regulatory domain (Fig. 2c). In the inactive state, a wide swing movement of PRD2 results in dimer opening and brings the phosphorylation sites to the protein surface. This movement is accompanied by additional structural rearrangements of both the PRD1-PRD1' interface and the CAT-PRD1 linker [8]. However, the structural information is available only for the N-terminal fragment with RAT (Fig. 2d); hence it failed to provide the complete interactions with protein [9]. Both the available protein–RNA complexes lack the information that is necessary to understand the activation as well as the overall mechanism; hence, we choose HutP protein for our study to reveal the complete anti-termination mechanism. The detailed analysis of this mechanism is described in this review.

2. Description of HutP system

HutP (Histidine utilizing Protein) is one of the anti-terminator proteins of *B. subtilis*, which is responsible for regulating the expression of the *hut* structural genes of this organism in response to changes in the intracellular levels of L-histidine [10,11]. In the *hut* operon, HutP is located just downstream from the promoter, while the five other subsequent structural genes, *hutH*, *hutU*, *hutI*, *hutG* and *hutM*, are positioned far downstream from the promoter [12–15]. In the presence of L-histidine and divalent metal ions, HutP binds to the nascent *hut* mRNA leader transcript. This allows the anti-terminator to form, thereby preventing the formation of the terminator and permitting transcriptional read-through into the *hut* structural genes. In the absence of L-histidine and divalent metal ions or both, HutP does not bind to the *hut* mRNA, thus allowing the formation of a stem loop terminator structure within the nucleotide sequence located between the *hutP* and structural genes [11]. Similarly to HutP, many regulatory proteins that involve allosteric regulation by small molecules to modulate protein binding to the cognate

mRNA have been described for various operons. For example, BglG, SacT and SacY, TRAP, PyrR, LacT, and GlpP regulate the *bgl*, *sac*, *trp*, *pyr*, *lac,* and *glp* operons, respectively [16–22]. These proteins must initially be activated by their specific ligands before they can function as anti-terminators/attenuators.

HutP is a 16.2 kDa protein consisting of 148 amino acid residues. HutP also exists in five other *Bacillus* species, including *Bacillus anthracis* [23], *Bacillus cereus* [24], *Bacillus halodurans* [25], *Bacillus thuringiensis* [26], and *Geobacillus kautophilus* [27], with 60% sequence identity. Sequence comparisons with the other *Bacillus* HutP proteins revealed that the C-terminal amino acid residues are more conserved than the N-terminal residues. Unlike other regulatory proteins, HutP not only requires L-histidine as the ligand but also divalent metal ions, by which this protein is distinguished from others.

3. Requirement of L-histidine

HutP requires L-histidine for binding to the *hut* mRNA [28]. Thus, L-histidine allosterically appears to control HutP–RAT interactions by modifying the conformational state of HutP. For the complete activation of HutP, a concentration of ~10 mM of L-histidine was sufficient for binding to the cognate RNA [28]. To obtain more insights into the requirement of L-histidine, we analyzed fifteen different L-histidine analogs to determine not only the functional groups responsible for activation but also to find the suitable analogs that exhibit higher affinity, using a filter-binding assay (Fig. 3). Among the analogs tested, L-histidine β-naphthylamide (HBN) and L-histidine benzylester showed higher affinity (Kd ~30 nM) over L-histidine (10-fold). L-histidine methyl ester and L-β-imidazole lactic acid showed similar affinity. L-histidine (Kd ~300 nM), urocanic acid, histamine, and L-histidinamide showed only weak activation. D-histidine, imidazole-4-acetic acid, L-histidinol, α-methyl–DL-histidine, 1-methyl L-histidine, 3-methyl L-histidine, and 3-2(thienyl)-L alanine, failed to show any activation [28,29].

Based on the analysis of the active analogs, we found that the imidazole group of L-histidine is very important for the activation. The attachment of a methyl group to the nitrogen/amide nitrogen

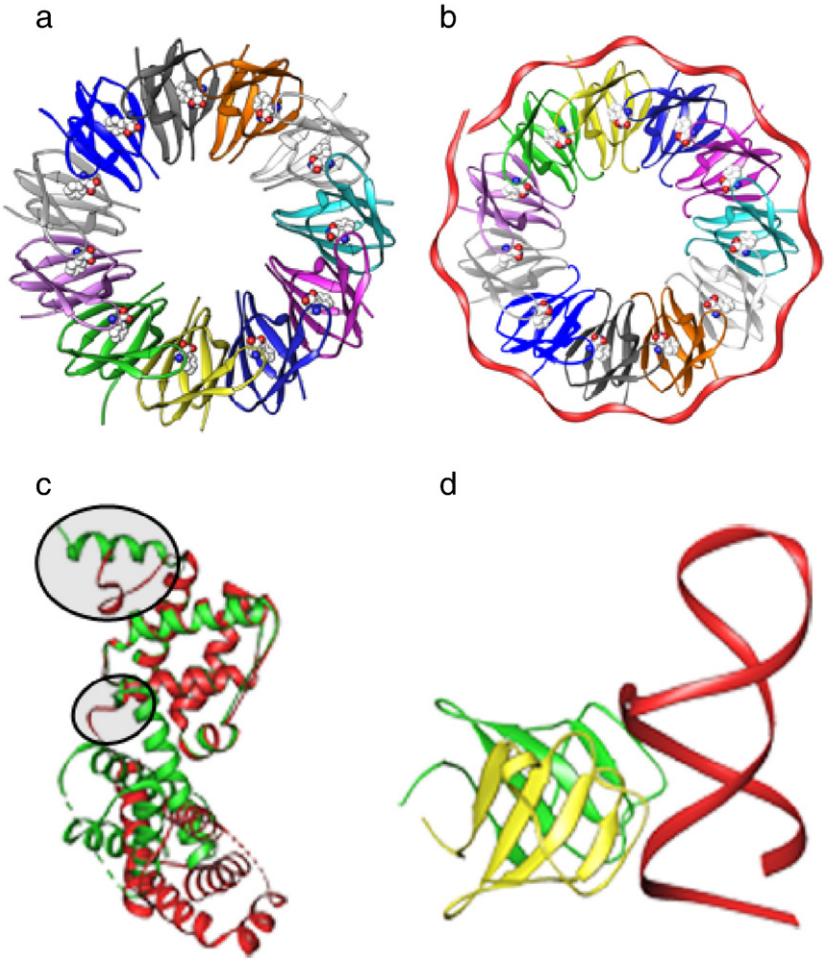

Fig. 2. Crystal structures of the known anti-terminator complexes. (a) Ribbon diagram of the binary complex of the TRAP (TRAP 11-mer bound with 11 tryptophan ligands); (b) ternary complex of the TRAP bound with 55-mer RNA containing 11 G(U)AG motifs. The L-tryptophan is shown in ball-and-stick format, and the bound RNA and proteins are shown in a ribbon diagram. (c) Structural comparison of the inactive (native, shown in green) and active (mutant, shown in red) LicT-PRD monomers superimposed onto PRD1. A significant conformational change is highlighted at the N-terminal and linker region. (d) The n-terminal fragment of the LicT protein in complex with a 29-mer RNA shows how the protein dimer stabilizes the RAT hairpin.

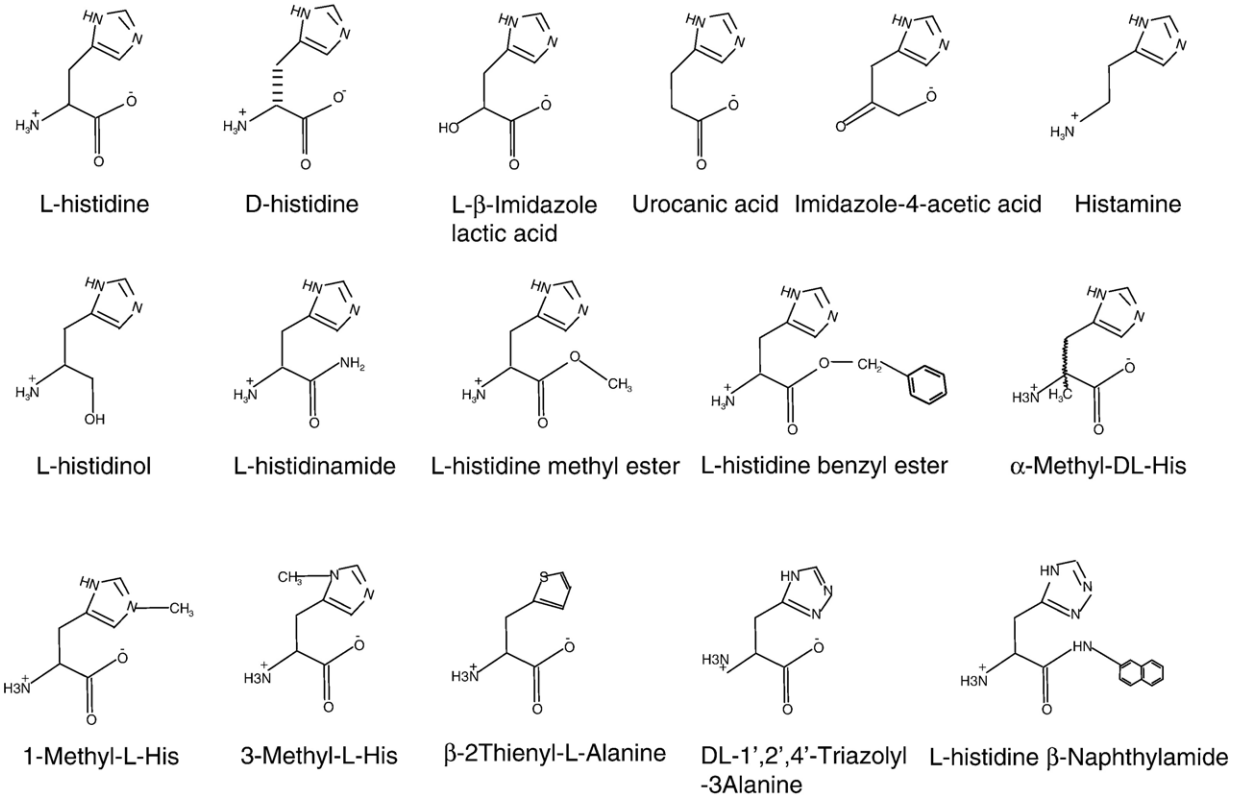

Fig. 3. Various L-histidine analogs used for the filter binding assay/gel mobility shift assay to evaluate the functional groups as well as the mode of activation.

of the imidazole group prevented *hut* mRNA binding, suggesting the importance of the imidazole group. Even though the results point to the importance of the imidazole ring of L-histidine in the activation of HutP, imidazole itself failed to activate the HutP protein, suggesting that the imidazole ring and the backbone moiety of L-histidine are essential for the activation. Moreover, the HutP activation by L-histidine is highly stereospecific because D-histidine prevented *hut* mRNA binding to the HutP protein, suggesting that the correct positioning of the α-amino and carboxy moieties of the L-histidine is essential.

4. Requirement of divalent metal ions

Our previous analyses suggested that the HutP protein binds to its cognate RNA only in the presence of L-histidine [28,30]. To analyze the ability of HutP to bind to the mRNA, the reactions are carried out in the presence of L-histidine (10 mM) and Mg^{2+} ions (10 mM). However, we do not know the importance of the metal ions in this anti-termination complex formation. To analyze the importance of the divalent metal ions in the formation of the HutP-L-histdine-RNA complex, we used a non-denaturing gel-shift assay to monitor the complex. HutP protein was dialyzed against binding buffer lacking $MgCl_2$ in order to remove the endogenous metal ions. When $MgCl_2$ was omitted from the binding reactions, HutP failed to bind to *hut* mRNA. When 0.5 mM of $MgCl_2$ was incorporated in the binding buffer, we clearly observed anti-termination complex formation. The amount of complex formation increased further with higher metal ion and L-histidine concentrations, and it displayed concentration dependence [31]. The divalent metal ion used in these studies (Kd ~489 μM) is also present in physiologically relevant concentrations in bacterial cells. The Kd value for the HutP–RNA interactions appeared to be more efficient (>10-fold) compared to the metal ions for other protein–RNA interactions, suggesting the existence of an efficient metal ion binding pocket. Therefore, HutP represents the first example of a single-stranded RNA-binding protein that requires metal ions for mediating RNA–protein interactions.

To substantiate further the requirement of divalent metal ions and also to evaluate the best divalent metal ions that support the interactions, we carried binding reactions in the presence of various monovalent (Na^+, K^+), divalent (Mg^{2+}, Ca^{2+}, Mn^{2+}, Cu^{2+}, Zn^{2+}, Co^{2+}, Cd^{2+}, Ba^{2+}, Sr^{2+}, Yb^{2+}, Ni^{2+}, Pb^{2+}, Ag^{2+}, Hg^{2+}, Pt^{2+}) metal ions [32]. Several divalent metal ions are found to mediate HutP–RNA interactions, in twelve out of fifteen divalent metal ions tested. The only metal ions that failed support are Cu^{2+}, Yd^{2+}, and Hg^{2+}. Among twelve divalent ions that support the interactions, Mn^{2+}, Zn^{2+}, and Cd^{2+}, are found to be the more efficient, followed by Mg^{2+}, Co^{2+}, and Ni^{2+} metal ions. Interestingly, the divalent metal ions that are less abundant in the bacterial cell, such as Mn^{2+}, Zn^{2+}, and Cd^{2+}, are found to be more active divalent metal ions, whereas divalent metal ions that represent in abundance (Mg^{2+}, Ag^{2+}, and Ca^{2+}) are found to be less efficient. Both of the monovalent cations (Na^+, K^+) failed to mediate the interactions even at the 10 mM and 100 mM concentrations in the absence of divalent cations.

These analyses conclude that the divalent cations are mandatory for the interactions and cannot be replaceable with monovalent cations [32].

5. Characterization of *hut* mRNA

The *hut* mRNA appears to form two alternative secondary structures that depend upon the presence of activated HutP protein [30]. The regions that fold into alternative structures are located between +459 and +572 of *hut* mRNA (Fig. 4). The *hut* mRNA appears to form a stable terminator structure (+498 to 572) in the absence of activated HutP, whereas the region between +459 and +537 seems to form a destabilized RNA structure (ribonucleic anti-terminator, RAT) upon binding to the activated HutP [30]. The minimal RAT that binds HutP was mapped previously to the nucleotide region from +459 to +537 of the *hut* mRNA. Our biochemical [30] and recent structural studies [28] revealed that HutP forms a hexamer, as a trimer of dimers. Based on these results, a search was made for repeated sequences within the minimal 79-mer RAT element, and three UAG repeats were found, each of which separated by a 4-nucleotide spacer region. To determine whether this is the HutP binding region, we synthesized a short RNA (21-mer-RAT) representing the region from +496 to +516 of the *hut* mRNA, and analyzed its binding to the activated HutP [28]. The equilibrium binding studies revealed that the 21-mer RAT (5′-CAUAGAUCUUAGACGAUAGGG-3′) binds to activated HutP as efficiently as the 79-mer RAT. Thus, the 21-mer RNA represents the minimal RNA element sufficient for HutP recognition. The bases located in the spacer regions between the UAG motifs could be replaced with other bases, but the four-nucleotide spacing was optimal for HutP recognition. If the spacer length decreased (2 nt and 3 nt), the UAG motif failed to reach the next binding site, while increasing the spacer length (5 nt and 6 nt) diminishes binding, suggesting that the extra nucleotides could cause the formation of a bulge, thereby allowing the spacing between the three docking sites to be maintained [28]. The gel mobility shift assays suggest that hexameric HutP has two potential binding sites for the cognate RNA. Based on these studies, the UAG appears to be the key motif for interactions with HutP. However, it was not clear whether the UAG motif (trimer RNA) alone is sufficient for HutP binding. To test this, we synthesized shorter RNAs: 3-mer (5′-UAG-3′), 4-mer (5′-AUAG-3′/5′-UAGA-3′), 7-mer (5′-UUUA-GUU-3′), and a 14-mer (5′-UUUAGUUUUUAGUU-3′) RNA containing either 3′ or 5′ phosphates, and analyzed them for binding to activated HutP [33]. None of the shorter RNAs, including the 7-mer, bound to HutP, whereas 14-mer RNA showed two-fold lower affinity as compared to that of the 21-mer RNA.

To substantiate further the importance of each of the bases, as well as to ascertain the tolerance for base substitutions in the UAG motif, we adopted an *in vitro* selection strategy as well as the site-specific mutational analyses [33]. Based on these experiments, identified 5′-UUUAGNNNNUAGNNNNUA-GUU-3′ as the recognition motif, where N indicates any base. These analyses further suggested that each HutP monomer recognizes one UAG motif, where the first base (U) can be substituted with other bases, while the second and third (A and G) are required for the interactions. The 6-amino of the A base and the 2-amino of the G base are the most important groups for the protein–RNA interactions, and the spacer nucleotides play no major role in these interactions. At least two UAG motifs are required for their cooperative interactions for protein–RNA recognition. In addition to this, the 2′-OH of A in the UAG motif was found to be very important for HutP recognition, based on the deoxyribose base substitutional analysis at the binding motif [32]. The stoichiometric analysis of HutP-RNA interactions through gel mobility shift assays confirmed that the hexameric HutP has two potential sites for RNA (1:2 ratio).

6. Crystal structures of HutP

The biochemical as well as the functional analysis of the HutP anti-termination complex suggests that the L-histidine, divalent metal ions, and an RNA containing the three NAG repeating motifs separated by four spacer nucleotides are mandatory for

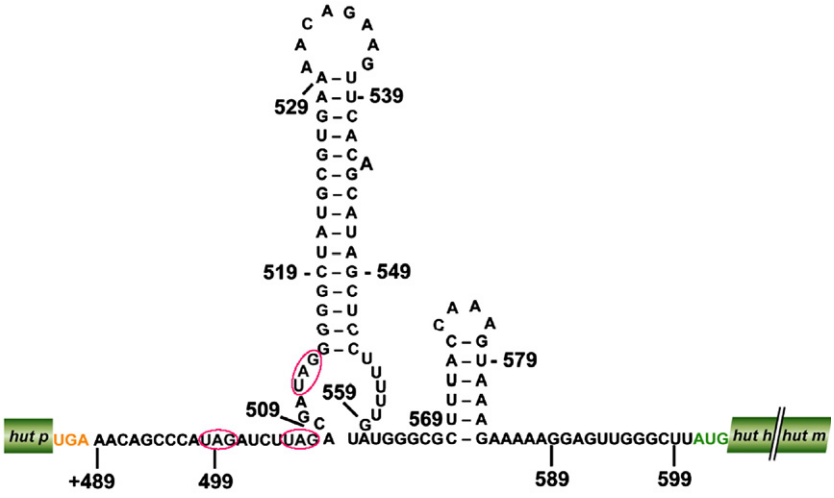

Fig. 4. The proposed *hut* mRNA terminator structure. The stop codon of the *hutP* gene and the start codon of the *hutH* gene are shown in orange and green, respectively. Within the HutP-recognition motif, the UAG motifs are highlighted with a red box.

the complex formation. In order to reveal the snap-shots of the complete mechanism of this HutP protein, we solved the crystal structures of the uncomplexed HutP [31], HutP–Mg^{2+} [33], HutP–L-histidine β-naphthylamide (HBN, an analog of L-histidine) [28,32], HutP–L-histidine–Mg^{2+} [31] and HutP–L-histidine–Mg^{2+}–21-mer RNA (UAG repeating motifs) [31,35]. In addition to these structures, an additional HutP–L-histidine–Mg^{2+}–21-mer RNA containing the three GAG repeats is presented here. This complex crystallized and solved the crystal structure as described previously [31,35]. All the data collection and refinement statistics are summarized in Table 1. The asymmetric unit (asu) of the uncomplexed HutP, HutP–Mg^{2+}, binary (HutP–HBN), quaternary complex-1 (HutP–L-histidine–Mg^{2+}–21-mer RNA containing UAG repeats), quaternary complex-2 (HutP–L-histidine–Mg^{2+}–21-mer RNA containing GAG repeats) contains two HutP molecules, whereas ternary complex (HutP–L-histidine–Mg^{2+}) contains 3 HutP molecules. All these asu dimers are related by three-fold and the trimers are related by a two-fold crystallographic symmetry to form a hexameric structure. The hexamer formation of HutP is important for the function, and it is consistent with the gel filtration assays. For ease of understanding, a dimer form of HutP is represented (Fig. 5). Each monomeric HutP molecule consisting of four α-helices and four β-strands, arranged in the order α-α-β-α-α-β-β-β in the primary structure, and the four antiparallel β-strands form a β-sheet in the order β1-β2-β3-β4, with two α-helices each on the front and the back. Although HutP belonged to the α/β family of proteins, a thorough search of PDB [36] and SCOP [37] databases revealed that HutP fold is novel and unrelated to any of the existing fold, as we expected, based on the sequence analysis of HutP protein as well as the RAT sequences.

Based on the structural analyses by superposition, uncomplexed HutP and HutP–Mg^{2+} display nearly similar conformations. The RMS deviations of superposition between these two structures were 0.80 Å. At the dimer interface, an open hydrophobic pocket is formed and stabilized by the salt bridge between the monomers of HutP, Glu81 of A and Arg88 of Molecule B. However, Mg^{2+} ions are not bound in the HutP–Mg^{2+} complex [31,32] (Fig. 5a).

Next, to determine the crystal structure of HutP with L-histidine, an analog of L-histidine, L-histidine β-naphthylamide (HBN), was used since it showed the highest affinity for the activation. The HutP protein co-crystallized with HBN and solved the structure [28,34]. The overall structure of this binary complex resembles the uncomplexed HutP (RMSD, 0.77) and HutP–Mg^{2+} (RMSD, 0.60) structures (Fig. 5b). An analog of L-histidine, HBN was bound between the monomers of HutP, and the imidazole group of

Table 1
Data collection and refinement statistics

	Uncomplexed HutP (Kumarevel et al., 2005a)	HutP–Mg^{2+} (Kumarevel et al., 2005b)	HutP–HBN (Kumarevel et al., 2004a)	HutP–L-His–Mg^{2+} (Kumarevel et al., 2005a)	HutP–L-His–Mg^{2+}–RNA (Kumarevel et al, 2005a)	HutP–L-His–Mg^{2+}–RNA (present work)
Data collection						
Space group	$P2_13$	$P2_13$	$P2_13$	$P2_12_12$	R3	R3
Cell dimensions (Å)	$a=b=c=96.82$	$a=b=c=95.41$	$a=b=c=95.41$, c=75.17	$a=77.79$, $b=80.88$,	$a=b=76.21$, $c=133.56$	$a=b=76.06$, $c=133.99$
No. of molecules/asymmetric unit	2	2	2	3	2	2
Resolution range (Å)	40.0–2.78 (2.88–2.78)[a]	20.0–2.60 (2.69–2.60)	20.0–2.80 (2.95–2.80)	50.0-1.70 (1.76–1.70)	50.0-1.60 (1.66–1.60)	50.0-1.48 (1.53–1.48)
Unique reflections	7867	8514	7379	52,114	38,063	47,155
Redundancy	5.8 (4.9)	12.2 (12.8)	7.1 (7.3)	6.3 (6.1)	3.9 (3.6)	5.6 (5.5)
Completeness (%)	98.8 (98.8)	93.1 (100)	100 (100)	96.5 (99.2)	99.8 (99.6)	97.5 (100)
R_{merge} (%)[b]	13.7 (30.0)	4.1 (35.0)	5.0 (23.9)	4.4 (26.0)	2.9 (25.8)	4.2 (31.4)
Refinement statistics						
Resolution range (Å)	20.0–2.80	20.0–2.70	20.0–2.80	20.0–1.70	20.0–1.60	20.0–1.48
Reflections used	7656	7492	7359	50,886	36,171	46,982
R (%)[c]	20.7	22.8	23.0	23.3	22.5	21.4
R_{free} (%)[d]	26.0	28.6	28.0	25.9	24.9	23.8
No. of protein atoms	2195	2144	2143	3285	2197	2218
No. of ligand atoms	0	0	21	33	22	22
No. of Mg^{2+} ions	0	0	0	3	2	2
No. of water molecules	92	67	84	578	314	405
Rmsd bond lengths (Å)	0.008	0.007	0.008	0.006	0.007	0.005
Rmsd bond angles (°)	1.5	1.3	1.4	1.3	1.3	1.20
PDB code	1WPS	1WPT	1VEA	1WPV	1WMQ[e]	1WPU[f]

[a]Values in parentheses are for the highest resolution shell.
[b]$R_{merge}=\sum_h \sum_i |I(h,i)-\langle I(h)\rangle| / \sum_h \sum_i (h,i)$, where $I(h,i)$ is the intensity value of the ith measurement of h and $\langle I(h)\rangle$ is the corresponding mean value of $I(h)$ for all i measurements.
[c]R factor $=\sum ||\mathbf{F}_{obs}|-|\mathbf{F}_{calc}|| / |\mathbf{F}_{obs}|$, where $|\mathbf{F}_{obs}|$ and $|\mathbf{F}_{calc}|$ are the observed and calculated structure factor amplitudes, respectively.
[d]R_{free} is the same as R factor, but for a 10% subset of all reflections.
[e]21-mer RNA containing UAG repeating motifs.
[f]21-mer RNA containing GAG repeating motifs.

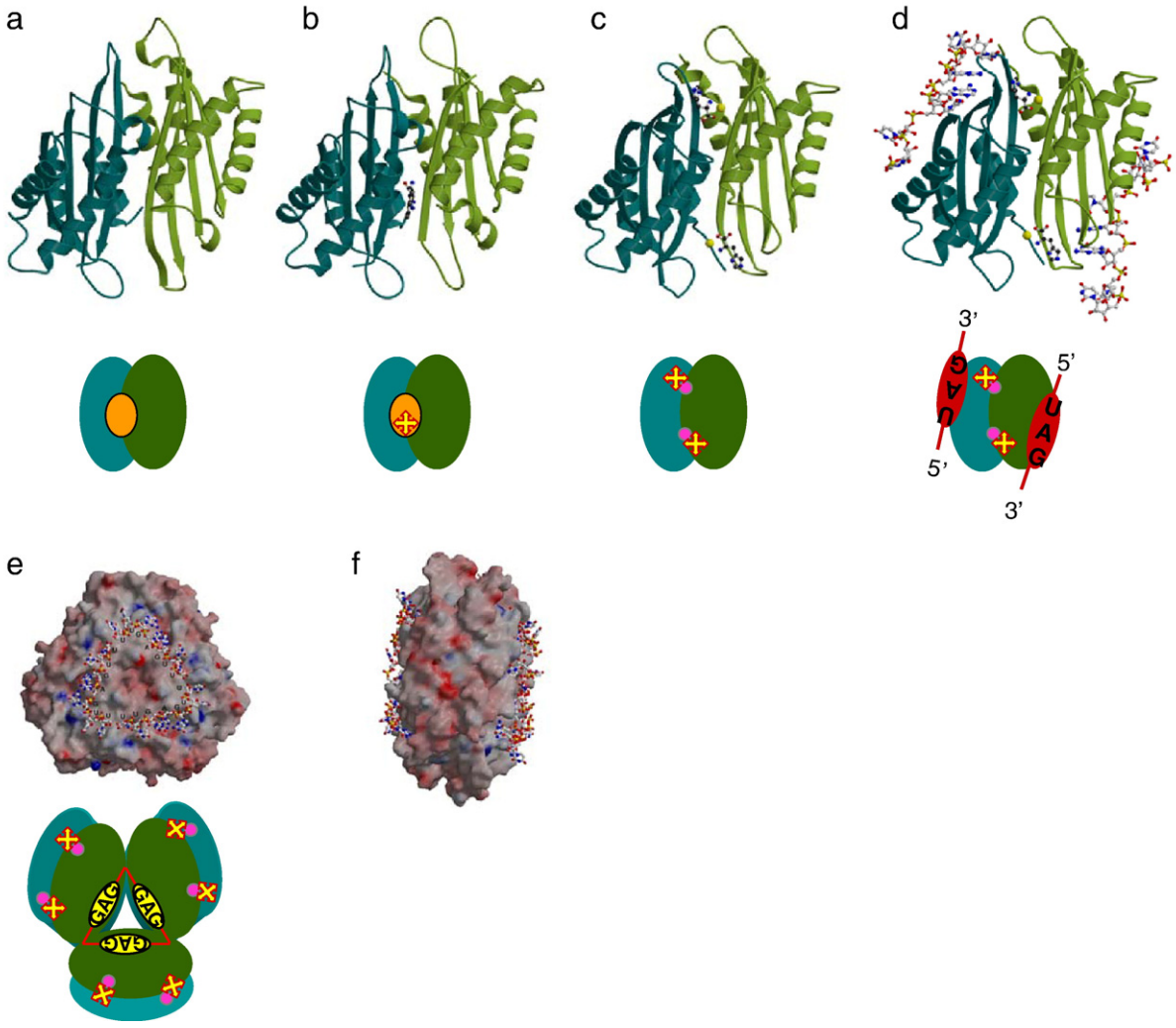

Fig. 5. Crystal structures of the HutP protein. (a) Structure of the uncomplexed HutP or HutP–Mg^{2+}; (b) Binary complex of HutP with L-histidine complex; (c) Ternary complex of HutP (HutP–L-histidine–Mg^{2+}). (d) Quaternary complex of HutP (HutP–L-histidine–Mg^{2+}–21-mer RNA). The biological assembly of HutP is a hexamer shown in surface representation in Figs. (e) and (f). The bound Mg^{2+} ions in ternary and quaternary complexes are represented by a cpk model. The bound RNA and the analog complexes (HBN in binary and L-histidine in ternary and quaternary) are shown in a ball-and-stick model. A schematic representation of the HutP dimer corresponding to the complexes is also shown under each figure.

L-histidine was buried in a hydrophobic pocket made up of two adjacent molecules. The imidazole ring amide nitrogen ND1 hydrogen-bonded with the side chain of Glu81 of the B molecule and the same Glu81 bonded to Arg88 through a salt bridge. The imidazole ring nitrogen (NE2) was hydrogen-bonded to the backbone moiety of Glu139 of molecule A and made another hydrophobic contact with the phenyl ring of Phe141 of molecule A. Mutational analyses of these critical residues suggested that the Glu81 and Arg88 were important for the analog interactions.

As shown in Fig. 5c, the HutP–L-histidine–Mg^{2+} (ternary) complex contained 2 L-histidines and 2 Mg^{2+} ions located on either side of the dimer interface [31,32]. The L-histidine imidazole ring projects downwards into the solvent, and the imidazole nitrogen (NE2) hydrogen bonds to a water molecule, while the amide nitrogen (ND1) hydrogen bonds to the side-chain oxygen of Tyr69 of the neighboring dimer within the HutP hexamer (Fig. 6, right upper panel). In contrast to the HutP–HBN complex, the amino (N) and carboxyl (CO and OXT) groups of the L-histidine backbone have many interactions. The carboxyl group forms a typical salt bridge with the guanidyl group of Arg88. In the HutP–HBN complex, this guanidyl group forms a typical salt bridge with the carboxyl group of Glu81 of molecule A, which is important for the formation of the hydrophobic pocket [28]. The amino group as well as the carboxyl group of L-histidine coordinates with the Mg^{2+} ion. The Mg^{2+} ion is involved in the formation of a typical six-coordination sphere. Of the six coordinations, three were with the imidazole nitrogens of His138, His73, and His77. The latter two histidines were those from the neighboring dimer. The sixth coordination of the Mg^{2+} ion was that with a water molecule, which was anchored by a hydrogen bond with the side chain of Glu81 of molecule A. To further substantiate the metal ion binding site residues on HutP, the residues that interact with the metal ions, His73, His77 and His138, were individually substituted with Ala, and the protein–RNA interactions were evaluated by a gel mobility shift assay [31]. These assays clearly showed that all three residues in the

histidine cluster were important for coordination with Mg^{2+} ion. Thus, the Mg^{2+} ion contributes toward mediating the interaction between HutP and L-histidine, along with the residues within the specific binding site in the dimer and the dimer-dimer interface of HutP. The recent crystal structures complexed with HutP–L-histidine-Mn^{2+} and HutP–L-histidine-Ba^{2+} revealed that the Mg^{2+} binding site can also accommodate different divalent cations, with ionic radii ranging from 0.72 to 1.35 Å, as suggested by the biochemical analysis [32].

The asymmetric unit of the quaternary complex-1 as well as the present quaternary complex-2, contains one homodimer of HutP, two L-histidines, two Mg^{2+} ions, and two 7-nucleotide fragments of the 21-mer RNA, which are related by a non-crystallographic two-fold axis [31,35] (Fig. 5d). In contrast to the quaternary complex-1, all the protein residues are clearly seen in quaternary complex-2. In the HutP dimer, L-histidine and Mg^{2+} ion are associated with each other, and are located in the dimer interface as observed in the HutP–L-histidine–Mg^{2+} complex. The bound L-histidine and Mg^{2+} ions recognized on one side of the HutP and the RNA on the other side. However, the Mg^{2+} ion does not bind directly to the RNA. This observation is in contrast with the role of metal ions reported in the past. For example, in the L11–RNA protein complexes, the metal ions occupy crucial locations to stabilize the sharp turns of the junctions, to strengthen the overall structure of the four-way junction [38]. The bound 21-mer RNA recognized on both the top and bottom surfaces of the HutP hexamer with a novel triangular fashion (Fig. 5e & f). Thus, the HutP hexamer recognizes two 21-mer RNA molecules, and this is consistent with our previous biochemical studies as suggested it predominantly forms 1:2 (Protein:RNA) complex ratios [28,33].

Each HutP monomer recognizes one unit of the 7-nucleotide fragment from the 21-mer RNA $(5'\text{-UUUAGUU-}3')_3$ passing across the β-sheet. In the 7-nucleotide RNA, the central A4-G5 forms an extensive hydrogen bonding network with HutP. The U7 interacts with the neighboring dimer within the HutP hexamer. Bases U1, U2 and U6 were partially disordered and showed no interactions with HutP. As U3 base observed in the quaternary complex-1, G3 base in the quaternary complex-2 also disordered and has no contact with the HutP. This analysis suggested that the U3 base is replaceable with other RNA bases, which is not important for the function and also consistent with our biochemical analysis [32]. The overall RNA structure adopts an extended A-RNA conformation, with C3′ endo sugar conformations for all of the residues. The central bases A4 and G5 are stacked upon each other, and the remaining bases probably serve as spacers without much interaction with the protein molecule; their basic requirement is apparently to place the next UAG binding site on the hexameric HutP.

No direct protein–RNA phosphate interactions were observed in the HutP ternary complex. The 2′-OH groups of the A4 and U7 sugars hydrogen-bonded with the side chains of Thr99 and Thr56, respectively. These two interactions involving the 2′-OH are critical for the protein–RNA interactions, which is consistent with the deoxyribo-nucleotide substitutional analysis [32] as well as the mutational analysis of the HutP protein. This explains the ability of HutP to distinguish between RNA and DNA. All of the hydrogen bonding interactions in this protein–RNA complex are mainly directed towards the base and the sugar, not the phosphate backbone, thus readily explaining the sequence-dependent nature of the recognition. To further substantiate the RNA binding site residues on HutP, the critical residues that interact with the RNA, Glu55, Thr56, Thr99, Thr128 and Glu137, were substituted with Ala, and the protein–RNA interactions were evaluated using both the gel mobility shift and filter binding assays. The Thr99Ala and Glu137Ala mutant proteins failed to bind to the RNA, while Glu55Ala (Kd 120±12 nM) and Thr56Ala (Kd 102±17 nM) mutants showed comparable affinities to the HutP protein (Kd 95±14 nM), whereas the binding ability for the Thr128Ala mutant was reduced by 15-fold (Kd 1431±480 nM). These studies clearly showed that residues Thr99 and Glu137 were completely responsible for RNA binding [31]. These analyses further suggested that the 2′-OH of the A4 ribose interaction with Thr99 was more important than the interaction of the 6-amino group of the A4 base with Thr128, and this was the reason why A4 could be substituted with U with 30-fold less affinity [33], owing to the loss of the 6-amino interactions with Thr128. These three residues are completely responsible for the RNA base-specific recognition. The other two residues, Glu55 and Thr56, have additional contacts with the spacer bases, but do not affect the overall binding or the complex structure formation. This analysis also supported our previous results and also our present complex with GAG repeats, which suggested that the spacer sequence only functions to provide spaces between the important bases in the *hut* mRNA.

It is interesting to compare the RNA conformations within both HutP and TRAP, because these two proteins recognize UAG motifs in their respective mRNAs. The overall conformations of these two RNAs are very different from each other; HutP recognizes two units of single-stranded RNA, forming a novel triangular shape, on both the top and bottom surfaces of the protein, whereas TRAP recognizes one unit of single-stranded RNA, forming a belt around the protein molecule [7]. The HutP requires UAG motifs separated by four spacer nucleotides, whereas the TRAP requires UAG/GAG motifs separated by two or three spacer nucleotides. The HutP RNA has an extended structure passing across the β-sheet along the HutP monomer, whereas the RNA is recognized in the dimer interface in the case of TRAP. Essentially, the A and G in the UAG motif are quite critical for the protein recognition in both HutP and TRAP. The RNA segment (A4-G5) recognized by HutP superimposes well on the A2-G3 of the RNA segment bound to TRAP, although their base orientations are slightly different from each other. The distinct feature shared by these two protein–RNA complexes is the absence of direct protein interactions with the RNA phosphates.

7. Allosteric activation of HutP by L-Histidine and Mg^{2+}

The overall structure of the HutP monomer has almost similar secondary structure in all our solved structures. However, the HutP–L-histidine–Mg^{2+}complex showed significant conformational changes when we superimpose on the

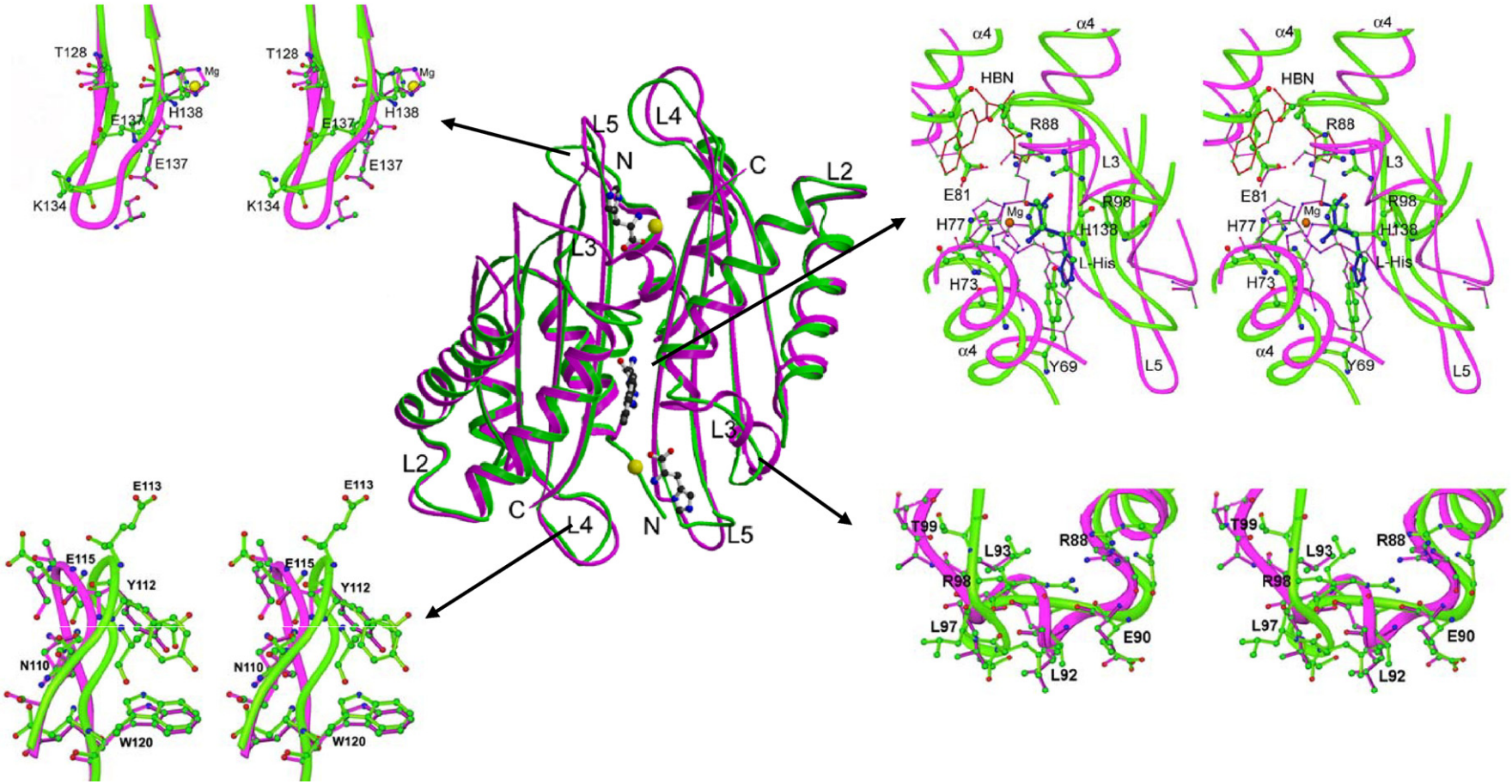

Fig. 6. Allosteric activation of the HutP protein. Superposition of two crystal structures (binary complex in pink; quaternary complex in green), showing the conformational changes at the L-histidine binding site and the loop regions L3, L4, and L5. The L-histidine β-naphthylamide and L-histidine are shown in a ball-and-stick model, and the Mg^{2+} ions are represented by a cpk model. Significant conformational changes observed in the L-histidine binding site, loop L3, L4, and L5 are magnified for easy viewing.

other structures, for uncomplexed HutP (rmsd, 3.1), HutP–Mg^{2+} (rmsd, 2.73), and HutP–HBN (rmsd, 3.15). The conformational changes observed especially at the L-histidine binding site and the loops, L3, L4 and L5 (Fig. 6). The uncomplexed HutP and HutP–Mg^{2+} structures clearly showed the existence of an open hydrophobic pocket at the dimer interface, and the HutP–HBN complex revealed that the imidazole group of the bound L-histidine ligand was completely buried inside the hydrophobic pocket and established the hydrogen binding network with the surrounding protein residues. In contrast to the previous structures, the HutP–L-histidine–Mg^{2+} complex distinctly showed the existence of two Mg^{2+}–L-histidine interactions on either side of the dimer interface. Based on this, it appeared that once the Mg^{2+} ion is bound by the HutP–L-histidine complex, the Mg^{2+} ion may pull the L-histidine out of the hydrophobic pocket and bind to it tightly. By this, the Mg^{2+}-bound L-histidine could move along the dimer interface and reside approximately 12 Å away from the pocket. This movement of L-histidine is apparently linked to the movement of Arg88 in the opposite direction, leading to the disruption of the hydrophobic pocket formed by the salt bridge between Arg88 and Glu81 in the HutP–HBN complex, and the formation of a new salt bridge between Arg88 and Arg98. This drastic rearrangement of Arg98 (C_α position shifted by 5.4 Å) is accompanied by a large change (5.0 Å) in the C_α position of the next residue, Thr99, of loop L3. On the other end, the re-orientation of the His138 imidazole ring to coordinate with the Mg^{2+} ion causes a large conformational change in the local backbone chain, particularly in the torsion angles around His138 and the next residue Glu137. Also the backbone oxygen of Glu137 bonded to the hydroxyl group of Try112. This changes the orientation of the sidechain of Glu137. Also, these changes in HutP might have been initiated by the Mg^{2+} ion and transmitted along the backbone chain to Thr128 through the L5 loop. In this complex, the metal ion and L-histidine mutually interact and facilitate the required overall structural rearrangement, because even if one of the two components (metal ion or L-histidine) is absent, HutP fails to bind to the RNA to form an anti-termination complex. However, L-histidine recognition must be the first step in this process, because until the imidazole ring of the L-histidine ligand is verified in the hydrophobic pocket, the HutP is not ready for the Mg^{2+} ion-mediated structural rearrangement. In the quaternary complex, protein did not go for further conformational changes upon binding to the RNA. Thus, both L-histidine and Mg^{2+} ions are responsible for the allosteric activation of HutP in HutP–L-histidine–Mg^{2+}complex, especially the conformational changes at the L-histidine binding site and Loops L3 and L5. The loop L3 responsible for critical interactions with 2′-OH of A4 base and the Loop L5 responsible for the 6-amino of A4 base and 2-amino of G5 bases in quaternary complex-1 [31] and the present quaternary complex-2. In the quaternary complex, the bound RNA undergoes the conformational change and showed a novel triangular fold in the hexameric HutP.

8. Unique mechanism of anti-termination

Based on analyses of the various biochemical and structural studies of HutP, a model proposed for the anti-termination of HutP [31,39] (Fig. 7). HutP protein forms hexamer in the presence or absence of ligands. Thus, HutP exists as a hexamer that forms a hydrophobic pocket in the center of each HutP dimer (step A). In the next step, the incoming residue is verified in the pocket, recognizes only the imidazole-containing residue (L-histidine) from the others, and then interacts extensively with the HutP residues in the pocket. This is the critical step for the selection of the ligands and also the selection is a stereospecific, because D-histidine fails to activate the HutP for the complex

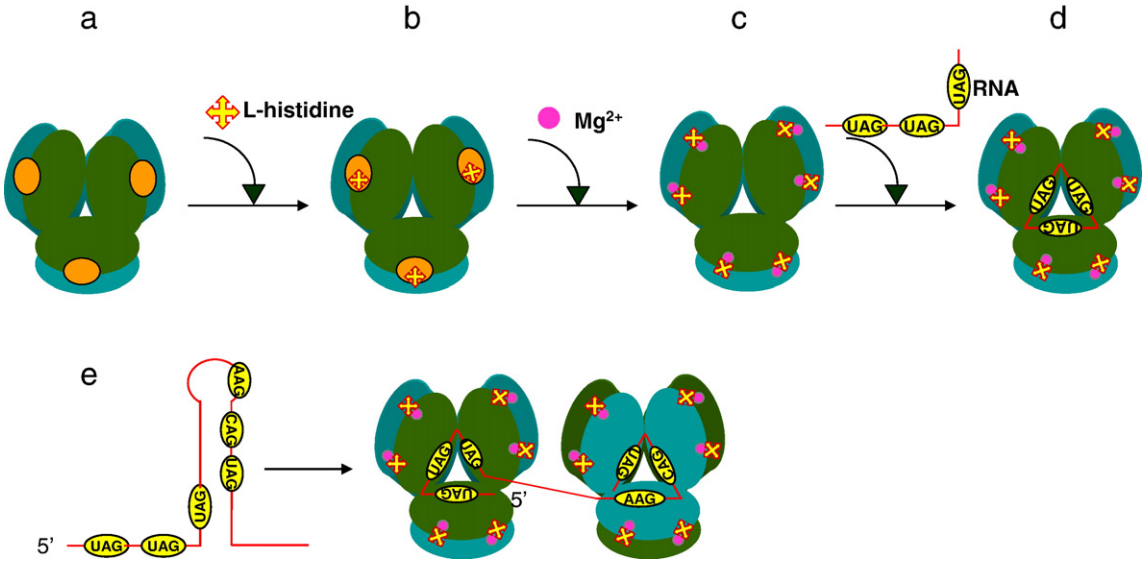

Fig. 7. Proposed schematic model for the HutP-antitermination mechanism. (a) Formation of HutP hexamer open hydrophobic pocket. (b) L-histidine recognition and discrimination with other ligands. (c) Allosteric activation of HutP in the presence of L-histidine and divalent metal ions, especially the L-histidine binding site and the loop regions L3, L4, and L5. (d) Recognition of RNA. (e) Schematic representation of a model proposed for the existence of two potential binding sites within the terminator region and the possible unwinding mechanism.

formation (step B). Once the L-histidine interactions have been completed in the pocket, HutP undergoes an allosteric activation in the presence of Mg^{2+} ions or other divalent metal ions, especially structural rearrangements at the L-histidine binding site and loops L3 and L5 (step C). This causes the L3 and L5 loops to specifically move and reorient the residues Arg88, Arg98, Thr99, Thr126, Glu137 and His138 for the RNA recognition. Once the HutP undergoes these conformational changes caused by the L-histidine and Mg^{2+} ions, then it recognizes the specific chemical groups of the bases within the *hut* mRNA, without undergoing any further structural rearrangement of the protein (step D), and the bound RNA may undergoes a conformational change.

The current structural and biochemical studies showed how the HutP allosterically activated in the presence of L-histidine and Mg^{2+} for the recognition *hut* mRNA. However, the present analyses have not revealed how the terminator structure is being altered to disrupt the stable structure. Also, we do not know the physiological relevance of the existence of two RNA binding sites in HutP. The reexamination of the entire intervening region between the *hutP* gene stop codon and the initiation codon of first structural gene, *hutH*, revealed the answers to those two questions. There are two potential binding sites (site I, +498 to +514; site II, +535 to +549) in the intervening sequence, and each binding site consists of three NAG motifs. Among these two, site I recognizes on one surface and the site II recognizes on the other surface of the hexameric HutP. A 20-nucleotide spacer region is present between the two binding sites, which is sufficient to reach site II on the other surface of the hexameric HutP (step E). From the 5′ end, the first binding site containing three NAG motifs separated by four nucleotides, whereas in the second binding site the third NAG motif separated by 2 nucleotide spacer. This may not affect the overall binding, because we showed previously that at least two NAG motifs are necessary to promote the RNA binding [33]. Based on these observations, we speculate that the hexameric HutP recognizes these two binding sites (I, II) of the *hut* mRNA on either side and by which the *hut* mRNA may undergo a complete destabilization of the terminator structure. Once the activated hutP recognizes the *hut* mRNA and destabilized the RNA, then RNA polymerase can easily pass through to transcribe the full-length genes.

9. Conclusions

Although many RNA-binding proteins are known to play a major role in regulating the gene expression by attenuation or anti-termination mechanism by targeting the nascent RNA only in the presence of their cognate ligands, however, no structural insights are yet available to understand the mechanism in each step. In order to fulfill this, the present review summarizes the recent structural and biochemical analysis of HutP and reveals how the HutP undergoes a conformational change in each step (apo-HutP, HutP–Mg^{2+}, HutP–L-histidine, HutP–Mg^{2+}–L-histidine, HutP–Mg^{2+}–L-histidine-RNA) to form an active anti-termination complex. Further structural and biochemical studies are required to understand the proposed model here, i.e., how the terminator structure is being destabilized upon binding to the activated HutP, which may help us further understand the anti-termination mechanism.

Acknowledgments

The author thanks Dr. P.K.R. Kumar and Dr. H. Mizuno for their kind encouragement and support during the HutP analysis work. The author also acknowledges Dr. Satoshi Nishikawa and staff personnel at beam-lines 6A and NW-12 at the Photon Factory for their help and encouragement.

References

[1] J.P. Richardson, J. Greenblatt, in: F.C. Neidhardt, R. Curtiss III, J.L. Ingraham, E.C.C. Lin, K.B. Low, B. Magasanik, W.S. Reznikoff, M. Riley, M. Schaechter, H.E. Umbarger (Eds.), *Escherichia coli* and *salmonella*: Cellular and Molecular Biology, American society for Microbiology, Washington, D. C., 1996, pp. 822–848.
[2] C. Yanofsky, Transcription attenuation: once viewed as a novel regulatory strategy, J. Bacteriol. 182 (2000) 1–8.
[3] P. Gollnick, P. Babitzke, Transcription attenuation, Biochim. Biophys. Acta 1577 (2002) 240–250.
[4] T.M. Henkin, Control of transcription termination in prokaryotes, Annu. Rev. Genet. 30 (1996) 35–57.
[5] B. Rutberg, Antitermination of transcription of catabolic operons, Mol. Microbiol. 23 (1997) 413–421.
[6] A.A. Antson, E.J. Dodson, G. Dodson, R.B. Greaves, X.P. Chen, P. Gollnick, Structure of the trp RNA-binding attenuation protein, TRAP, bound to RNA, Nature 401 (1999) 235–242.
[7] A.A. Antson, J. Otridge, A.M. Brzozowski, E.J. Dodson, G.G. Dodson, K.S. Wilson, T.M. Smith, M. Yang, T. Kurecki, P. Gollnick, The structure of trp RNA-binding attenuation protein, Nature 374 (1995) 693–700.
[8] M. Graille, C.Z. Zhou, V.R. Brechot, B. Collinet, N. Declerck, H. Van ilbeurgh, Activation of the LicT transcriptional antiterminator involves a domain swing/lock mechanism provoking massive structural changes, J. Biol. Chem. 280 (2005) 14780–14789.
[9] Y. Yang, N. Declerck, X. Manivel, S. Aymerich, M. Kochoyan, Solution structure of the LicT-RNA antitermination complex: CAT clamping RAT, EMBO J. 21 (2002) 1987–1997.
[10] M. Oda, T. Katagai, D. Tomura, H. Shoun, T. Hoshino, K. Furukawa, Analysis of the transcriptional activity of the hut promoter in *Bacillus subtilis* and identification of a cis-acting regulatory region associated with catabolite repression downstream from the site of transcription, Mol. Microbiol. 6 (1992) 2573–2582.
[11] L.V. Wray Jr., S.H. Fisher, Analysis of *Bacillus subtilis* hut operon expression indicates that histidine-dependent induction is mediated primarily by transcriptional antitermination and that amino acid repression is mediated by two mechanisms: regulation of transcription initiation and inhibition of histidine transport, J. Bacteriol. 176 (1994) 5466–5473.
[12] L.A. Chasin, B. Magasanik, Induction and repression of the histidine-degrading enzymes of *Bacillus subtilis*, J. Biol. Chem. 243 (1968) 5165–5178.
[13] Y. Kimhi, B. Magasanik, Genetic basis of histidine degradation in *Bacillus subtilis*, J. Biol. Chem. 245 (1970) 3545–3548.
[14] M. Oda, A. Sugishita, K. Furukawa, Cloning and nucleotide sequences of histidase and regulatory genes in the *Bacillus subtilis* hut operon and positive regulation of the operon, J. Bacteriol. 170 (1988) 3199–3205.
[15] K. Yoshida, H. Sano, S. Seki, M. Oda, M. Fujimura, Y. Fujita, Cloning and sequencing of a 29 kb region of the *Bacillus subtilis* genome containing the hut and wapA loci, Microbiology 141 (1995) 337–343.
[16] F. Houman, M.R. Diaz-Torres, A. Wright, Transcriptional antitermination in the bgl operon of *E. coli* is modulated by a specific RNA binding protein, Cell 62 (1990) 1153–1163.
[17] S. Aymerich, M. Stenmetz, Specificity determinants and structural features in the RNA target of the bacterial antiterminator proteins of the BglG/SacY family, Proc. Natl. Acad. Sci. U. S. A. 89 (1992) 10410–10414.

[18] P. Babitzke, C. Yanofsky, Reconstitution of *Bacillus subtilis* trp attenuation in vitro with TRAP, the trp RNA-binding attenuation protein, Proc. Natl. Acad. Sci. U. S. A. 90 (1993) 133–137.
[19] M.D. Arnaud, M. Debarbouille, G. Rapoport, M.H. Saier Jr., J. Reizer, In vitro reconstitution of transcriptional antitermination by the SacT and SacY proteins of *Bacillus subtilis*, J. Biol. Chem. 271 (1996) 18966–18972.
[20] Y. Lu, R.J. Turner, R.L. Switzer, Function of RNA secondary structures in transcriptional attenuation of the *Bacillus subtilis* pyr operon, Proc. Natl. Acad. Sci. U. S. A. 93 (1996) 14462–14467.
[21] C.A. Alpert, U. Siebers, The lac operon of *Lactobacillus casei* contains lacT, a gene coding for a protein of the Bg1G family of transcriptional antiterminators, J. Bacteriol. 179 (1997) 1555–1562.
[22] E. Glatz, R.P. Nilsson, L. Rutberg, B. Rutberg, A dual role for the *Bacillus subtilis* glpD leader and the GlpP protein in the regulated expression of glpD: antitermination and control of mRNA stability, Mol. Microbiol. 19 (1996) 319–328.
[23] T.D. Read, S.N. Peterson, N. Tourasse, L.W. Baillie, I.T. Paulsen, K.E. Nelson, H. Tettelin, D.E. Fouts, J.A. Eisen, S.R. Gill, et al., The genome sequence of *Bacillus anthracis Ames* and comparison to closely related bacteria, Nature 423 (2003) 81–86.
[24] N. Ivanova, A. Sorokin, I. Anderson, N. Galleron, B. Candelon, V. Kapatral, A. Bhattacharyya, G. Reznik, N. Mikhailova, A. Lapidus, et al., Genome sequence of *Bacillus cereus* and comparative analysis with *Bacillus anthracis*, Nature 423 (2003) 87–91.
[25] H. Takami, K. Nakasone, Y. Takaki, G. Maeno, R. Sasaki, N. Masui, F. Fuji, C. Hirama, Y. Nakamura, N. Ogasawara, et al., Complete genome sequence of the alkaliphilic bacterium *Bacillus halodurans* and genomic sequence comparison with *Bacillus subtilis*, Nucleic Acids Res. 28 (2000) 4317–4331.
[26] T.S. Brettin, D. Bruce, J.F. Challacombe, P. Gilna, C. Han, K. Hill, P. Hitchcock, P. Jackson, P. Keim, J. Longmire, S. Lucas, R. Okinaka, P. Richardson, E. Rubin, H. Tice, "Complete genome sequence of *Bacillus thuringiensis* 97–27" Submitted for publication (JUN-2004) to the EMBL/GenBank/DDBJ databases.
[27] H. Takami, Y. Takaki, G.J. Chee, S. Nishi, S. Shimamura, H. Suzuki, S. Matsui, I. Uchiyama, Thermoadaptation trait revealed by the genome sequence of thermophilic *Geobacillus kaustophilus*, Nucleic Acids Res. 32 (2004) 6292–6303.
[28] T.S. Kumarevel, Z. Fujimoto, P. Karthe, M. Oda, H. Mizuno, P.K.R. Kumar, Crystal structure of activated HutP; an RNA binding protein that regulates transcription of the hut operon in *Bacillus subtilis*, Structure 12 (2004) 1269–1280.
[29] T.S. Kumarevel, H. Mizuno, P.K.R. Kumar, Allosteric activation of HutP protein, that regulates transcription of hut operon in *Bacillus subtilis*, mediated by various analogs of histidine, Nucleic Acids Res. Suppl. 3 (2003) 199–200.
[30] M. Oda, N. Kobayashi, A. Ito, Y. Kurusu, K. Taira, cis-acting regulatory sequences for antitermination in the transcript of the *Bacillus subtilis* hut operon and histidine-dependent binding of HutP to the transcript containing the regulatory sequences, Mol. Microbiol. 35 (2000) 1244–1254.
[31] T.S. Kumarevel, H. Mizuno, P.K.R. Kumar, Structural basis of HutP-mediated anti-termination and roles of the Mg^{2+} ion and L-histidine ligand, Nature 434 (2005) 183–191.
[32] T.S. Kumarevel, H. Mizuno, P.K.R. Kumar, Characterization of the metal ion binding site in the anti-terminator protein, HutP, of *Bacillus subtilis*, Nucleic Acids Res. 33 (2005) 5494–5502.
[33] T.S. Kumarevel, S.C.B. Gopinath, S. Nishikawa, H. Mizuno, P.K.R. Kumar, Identification of important chemical groups of the hut mRNA for HutP interactions that regulate the hut operon in *Bacillus subtilis*, Nucleic Acids Res. 32 (2004) 3904–3912.
[34] T.S. Kumarevel, Z. Fujimoto, B. Padmanabhan, M. Oda, S. Nishikawa, H. Mizuno, P.K.R. Kumar, Crystallization and preliminary X-ray diffraction studies of HutP protein: an RNA-binding protein that regulates the transcription of hut operon in *Bacillus subtilis*, J. Struct. Biol. 138 (2002) 237–240.
[35] T.S. Kumarevel, Z. Fujimoto, H. Mizuno, P.K.R. Kumar, Crystallization and preliminary X-ray diffraction studies of the metal-ion-mediated ternary complex of the HutP protein with L-histidine and its cognate RNA, BBA-Proteins Proteomics 1702 (2004) 125–128.
[36] H.M. Berman, T. Battistuz, T.N. Bhat, W.F. Bluhm, P.E. Bourne, K. Burkhardt, Z. Feng, G.L. Gilliland, L. Iype, S. Jain, P. Fagan, J. Marvin, D. Padilla, V. Ravichandran, B. Schneider, N. Thanki, H. Weissig, J.D. Westbrook, C. Zardecki, The protein data bank, Acta Crystallogr., D. Biol. Crystallogr. 58 (2002) 899–907.
[37] A.G. Murzin, S.E. Brenner, T. Hubbard, C. Chothia, SCOP: a structural classification of proteins database for the investigation of sequences and structures, J. Mol. Biol. 247 (1995) 536–540.
[38] B.T. Wimberly, R. Guymon, J.P. McCutcheon, S.W. White, V. Ramakrishnan, A detailed view of a ribosomal active site: the structure of the L11–RNA complex, Cell 97 (1999) 491–502.
[39] P.K.R. Kumar, T.S. Kumarevel, H. Mizuno, Structural basis of HutP-mediated transcription anti-termination, Curr. Opin. Struct. Biol. 16 (2006) 18–26.